1 **Transient CRISPR immunity leads to coexistence with phages**

2

3 Sean Meaden[1]*, Loris Capria[1], Ellinor Alseth[1], Ambarish Biswas[2], Luca Lenzi[3], Angus

4 Buckling[1], Stineke van Houte[1], Edze R Westra[1]*

5

6 1. Biosciences, University of Exeter, TR10 9EZ, UK

7 2. Department of Microbiology and Immunology, University of Otago, Dunedin, New

8 Zealand

9 3. Institute of Integrative Biology, University of Liverpool, L69 7ZB, UK

10 *corresponding authors

11 email: s.meaden@exeter.ac.uk; e.r.westra@exeter.ac.uk

12

13

14   ***Abstract***

15   Phages play a major role in shaping the composition, evolution and function of bacterial

16   communities. While bacteria and phages coexist in many natural environments, their

17   coexistence is often short-lived in the lab due to the evolution of phage resistance. However,

18   fitness costs associated with resistance and mutational loss of resistance alleles may limit the

19   durability of acquired resistances, potentially allowing phages to re-invade the population.

20   Here, we explore this idea in the context of bacteria that evolve CRISPR-based immunity

21   against their phages. Consistent with previous studies, we found that the bacterium

22   *Pseudomonas aeruginosa* PA14 evolved high levels of CRISPR-based immunity and low

23   levels of surface-based resistance following infection with phage DMS3vir, which led to

24   rapid phage extinction. However, when these pre-immunized bacterial populations were

25   subsequently challenged with the same phage, they failed to clear the infection and instead

26   stably coexisted with the phage. Analysis of bacterial genotypes and phenotypes over time

27   explained why CRISPR-Cas immunity provides only a transient advantage: in the absence of

28   phage (i.e. following the initial phage extinction) formerly CRISPR-immune bacteria regain

29   sensitivity due to evolutionary loss of spacers, whereas in the presence of phage (i.e. upon

30   reinfection) selection favours surface-based resistance over CRISPR immunity. The latter

31   results from an infection-induced fitness cost of CRISPR-immunity that is due to phage gene

32   expression prior to target DNA cleavage by the immune system. Together, these results show

33   that CRISPR-Cas immune systems provide only a transient benefit to bacteria upon phage

34   infection and help to explain why bacteria and phages can coexist in natural environments

35   even when bacteria carry CRISPR-Cas adaptive immune systems that allow for rapid

36   acquisition of immunity against phages.

37

38

39   *Main*

40   Phages are ubiquitous in prokaryotic communities and play a vital role in key ecological

41   processes. For example, phage predation may cause up to 20% of mortality of all bacteria in

42   the world's oceans, making them key players in global nutrient cycling (Suttle 2007). In the

43   deep terrestrial biosphere, phages regulate microbial communities- in turn shaping resource

44   turnover (Daly *et al.* 2019) and in wetland ecosystems, phages have been associated with

45   regulation of methanogens and sulfate reducers (Dalcin Martins *et al.* 2018). In addition to

46   ecological processes, co-evolution between phages and bacteria can generate and accelerate

47   increases in bacterial and phage genetic diversity (van Houte *et al.*; Paterson *et al.* 2010;

48   Scanlan *et al.* 2015), mediate horizontal gene transfer (Canchaya *et al.* 2003) and alter

49   competition among bacteria (reviewed in Koskella & Brockhurst 2014). As well as this

50   important ecological role, phages are also increasingly seen as a promising alternative to

51   antibiotics to treat bacterial infections of plants, animals and humans (Wagenaar *et al.* 2005;

52   Balogh *et al.* 2010; Kutter *et al.* 2010). Therefore, understanding the factors that shape the

53   ecology and evolution of bacteria-phage interactions is fundamentally important.

54

55   The impact of phages on bacterial species and communities in ecological and biomedical

56   settings is inevitably constrained by both pre-existing (innate) and acquired phage resistance

57   (reviewed in Labrie *et al.* 2010). Bacteria can acquire phage resistance either by mutation or

58   masking of the cell surface receptors to which the phages bind, or through their adaptive

59   immune systems known as CRISPR-Cas (Clustered Regularly Interspaced Short Palindromic

60   Repeats; CRISPR-associated). CRISPR-Cas works by inserting phage-derived sequences into

61   CRISPR loci on the host genome, which function as genetic memory to detect and destroy

62   phages carrying the same sequence (reviewed in Marraffini 2015). This can lead to rapid

63   phage extinction, as phages are effectively being actively removed from the environment (as

64   opposed to surface-based resistance where phages persist in the environment).

65

66   While CRISPR immunity can drive phages extinct in the short term, it is less clear how this

67   immune system impacts phage persistence in the long term. Given that acquired resistance

68   alleles are heritable, one would perhaps expect that pre-immunized bacterial populations

69   would remain fully resistant to reinfection by the same phage genotype. On the other hand,

70   there may be selection against CRISPR immunity due to costs in the form of autoimmunity

71   (Stern *et al.* 2010), or if CRISPR is less effective under high phage exposure (Westra *et al.*

72   2015). Additionally recent theory and data suggest that individual bacteria may lose their

73   CRISPR-resistance due to mutations in the *cas* genes or CRISPR arrays (Weissman *et al.*

74   2019).

75

76   To test the durability of CRISPR-based immunity, we recurrently infected *Pseudomonas*

77   *aeruginosa* PA14 with phage DMS3vir (Cady *et al.* 2012), a mu-like phage (Budzik *et al.*

78   2004). By sequentially re-introducing the phage at different time intervals we vary the

79   intensity of selection for resistance (surface mutation) and immunity (CRISPR) and track the

80   resulting ecological dynamics. By using a combination of experimental evolution and

81   genomic analyses we tease apart the population genetics that underpin this host-parasite

82   interaction. These results have implications for how genetic diversity can be both generated

83   and lost in bacterial populations and help explain the coexistence of bacteria and phages in

84   natural microbial communities.

85

86

87

88 ***Results***

89 *Populations lose the ability to drive phages extinct*

90 CRISPR mediated immunity acts as an acquired, heritable genetic memory against phages

91 (Marraffini 2015), however the timescales over which it is effective are unknown. Based on

92 our mechanistic understanding of CRISPR immunity, one would predict that population-level

93 immunity is long-lived. However, the few empirical studies that directly measure population

94 and evolutionary dynamics of CRISPR-phage interactions have either focussed on short-term

95 dynamics (Westra *et al.* 2015; van Houte *et al.* 2016) or examined CRISPR in isolation

96 (Paez-Espino *et al.* 2013; Common *et al.* 2019), rather than the interplay between alternative

97 resistance strategies. Recent theory and data suggests that resistance alleles may be lost from

98 bacterial populations due to back mutations towards a sensitive phenotype when resistance is

99 costly, which can in turn allow for phage persistence (Weissman *et al.* 2018; Chaudhry *et al.*

100 2018; Gurney *et al.* 2019). To test this, we exposed *P. aeruginosa* PA14, which carries a type

101 I-F CRISPR system, to phage DMS3vir, which carries a mutation in its repressor gene that

102 prevents lysogeny, as well as a partial protospacer match which promotes primed spacer

103 acquisition by *P. aeruginosa* PA14 (Westra *et al.* 2015). We then measured whether

104 populations could repeatedly drive phage DMS3vir to extinction following an initial phage

105 exposure. Consistent with earlier findings, following the first infection treatment, phage titers

106 were found to initially increase due to the phage epidemic that takes place in the sensitive

107 bacterial population, followed by a rapid decline in phage titers and extinction at 4 days post

108 infection (dpi) (Fig. 1A), due to the evolution of CRISPR-based immunity in the bacterial

109 population (van Houte *et al.* 2016 and Fig. 2). To test whether these now immunized bacteria

110 could survive subsequent infections they were reinfected with 10^7 pfu phage at 5 dpi.

111 Consistent with the bacterial population having evolved CRISPR-mediated phage resistance

112 in response to the earlier phage challenge the phage was rapidly driven to extinction (Fig.

113   1B). Strikingly, when the same bacterial populations were re-infected 5 days later (at 10 dpi)

114   they had lost the ability to drive the phage extinct (Fig. 1B), and phage was able to persist for

115   the remainder of the 30-day experiment in all replicates of the same treatment. Similarly, in

116   the treatment where the first re-infection took place at 10 dpi, the bacterial populations also

117   had lost the ability to drive phage extinct (Fig. 1C). As expected, the treatment where phage

118   was added every day showed high phage titres throughout the experiment (Fig. 1D), and in

119   the phage-free treatment no phage could be detected (data not shown).
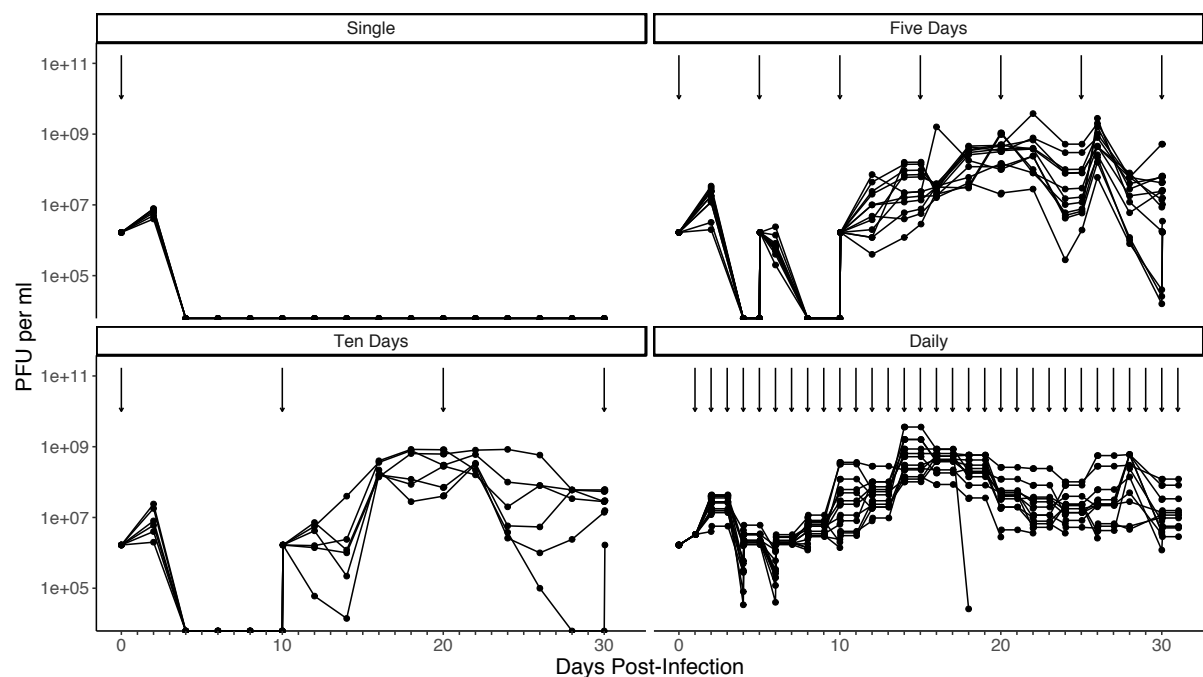
120
121
122

123

124

125   Figure 1. Phage titres over time upon infection of *P. aeruginosa* with DMS3vir. Arrows

126   denote timing of reinfection, each line represents an individual replicate population. A) No

127   reinfection (n = 6). B) Reinfection every 5 days (n = 12). C) Reinfection every 10 days (n =

128   6). D) Daily reinfection. (n = 12). Phage titres were recorded every 2 days. Note this figure

129   includes imputed values for non-recorded days that combine the previous days titre with the

130   phages that were added. Limit of detection is 200 PFU per ml.

131

Populations are invaded by surface resistance mutants and sensitive clones

133   To understand why phages can successfully re-infect populations that previously drove the

134   same phage extinct, we phenotypically characterised the composition of the host populations,

135   i.e. the proportion of sensitive bacteria as well as the proportion of bacteria that had acquired

136   at least one new spacer that conferred CRISPR-based immunity (CRISPR-immune herein) or

137   surface mutation based resistance (i.e. bacteria that evolved phage resistance through loss or

138   masking of the phage receptor, SM herein). At 4 dpi 0.66 ± 0.036 (mean proportion $\pm$ SE) of

139   bacteria in the populations from the single infected treatment evolved CRISPR-immunity,

140   0.25 ± 0.040 evolved SM resistance, and 0.083 ± 0.022 remained sensitive. At 30 dpi, these

141   fractions had changed to 0.0069 ± 0.0069 CRISPR immunity, 0.38 ± 0.073 SM, and $0.61 \pm$

142   0.73 sensitives. The invasion of sensitive bacteria in the absence of phage suggests that either

143   CRISPR immunity is associated with a constitutive fitness cost, or that there is back mutation

144   from CRISPR immunity to the sensitive, ancestral genotype (examined in detail later).

145   Next, to understand how the reinfection regimes impact the evolutionary dynamics of

146   the host population, we examined how the evolution of CRISPR immunity and surface

147   resistance varied across our treatments. At 4 dpi, we found an interaction between the

148   proportion of each phenotype and reinfection frequency (GLM, $F1, 102 = 7.06$, $p < 0.0001$),

149   with populations that were re-infected daily had slightly increased levels of SM compared to

150   those only infected once ($F_{1,35} = 17.94$, $p < 0.001$), which is consistent with previous results

151   that demonstrate a shift towards SM when phage exposure is high (Westra *et al.* 2015).

152   Interestingly, for all treatments, we observed a significant reduction in CRISPR-immune

153   clones over time (quasibinomial GLM, $F_{1,22} = 179.8$, $p < 0.0001$), but no interaction between

154   treatment and time (quasibinomial GLM, $F_{1,16} = 2.4$, $p = 0.16$), suggesting the reinfection

155   regime was not driving the observed decline. However, while in the single infection treatment

156   the decline in CRISPR-immune clones was due to the invasion of sensitive bacteria, we

157   observed invasion of surface resistant bacteria in the reinfection treatments instead (Fig. 2).
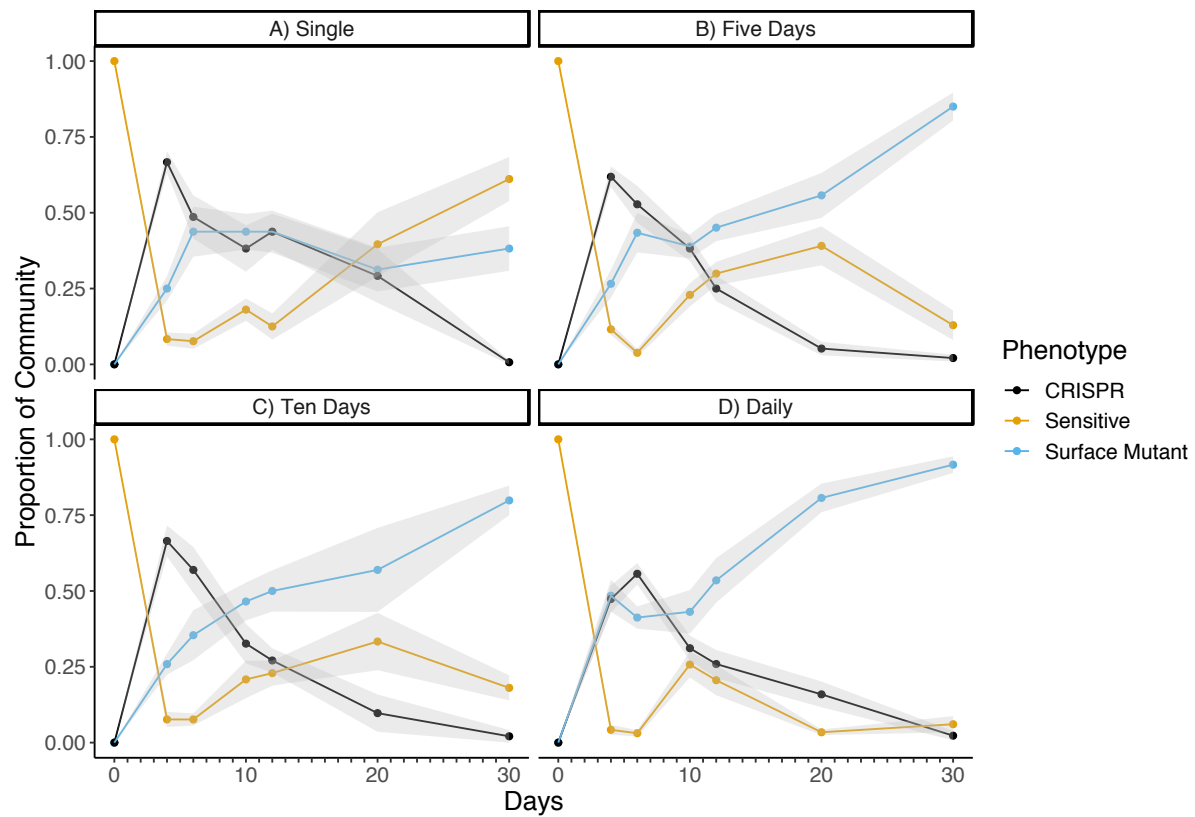

158

159   Figure 2. Frequencies of phage resistant and sensitive phenotypes. A) No reinfection, n = 6

160   B) Reinfection every 5 days, n = 12 C) Reinfection every 10 days, n = 6, 5D) Daily

161   reinfection, n = 12. Proportions were determined from phenotypic assays of 24 clones per

162   population. Lines represent the means across populations and shaded areas represent ±1

163   SEM. CRISPR-immune bacteria are shown in black, bacteria with surface-based resistance in

164   blue, and clones that remain sensitive to the phage in yellow.

165

166   *The population genetics of phage resistance and immunity*

167   These phenotypic data were further supported by genotypic data. First, we sequenced the

168   genomes of a single SM clone from each population at day 12. Consistent with phage

169   DMS3vir being pilus-specific (Budzik *et al.* 2004), we identified in all cases a SNP in a pilus

170   affiliated gene (PilC, PilB, PilQ, PilY1), a deletion of the PilM gene or, most frequently, a

171   10kb deletion of 7 pilus-associated genes (at position 5948050 – 5958338; Fig. 3, panel E),

172   which was identical in all independent isolates and hence suggests these areas of the genome

173   contain sequences with microhomology that are prone to recombination. In addition, we

174   carried out deep sequencing of CRISPR array amplicons (CRISPR1 and CRISPR2) of all

175   experimental populations. This demonstrated an extremely high spacer diversity (133249

176   unique CRISPR arrays) that is sufficient to cover all 5643 possible target sequences on the

177   phage genome (Fig.S1). We found a significant interaction between time and reinfection

178   frequency, with spacer diversity declining in all groups with the exception of populations that

179   were infected daily, which maintained spacer diversity for longer (GLM, $F_{1,85} = 6.65$, p <

180   0.001, with qualitatively similar results for Shannon's or Simpson's diversity indices).

181   Moreover, the frequency of array sequences lacking any new spacers increased over time

182   (GLM, $F_{1,89} = 228$, p < 0.0001), as would be expected given the invasion of sensitive and SM

183   clones. Interestingly, arrays with multiple spacers all declined throughout the experiment (up

184   to 5 spacers, Fig 3, Panel A). When we tracked the fates of individual spacers (in order to

185   identify variation in spacer effectiveness) we typically found a consistent decline in spacer

186   abundance, with only a few exceptions (Fig 3, panel B) that most likely represent CRISPR

187   immune clones that subsequently acquired a surface mutation (Fig. 3, Panel C).

188

189
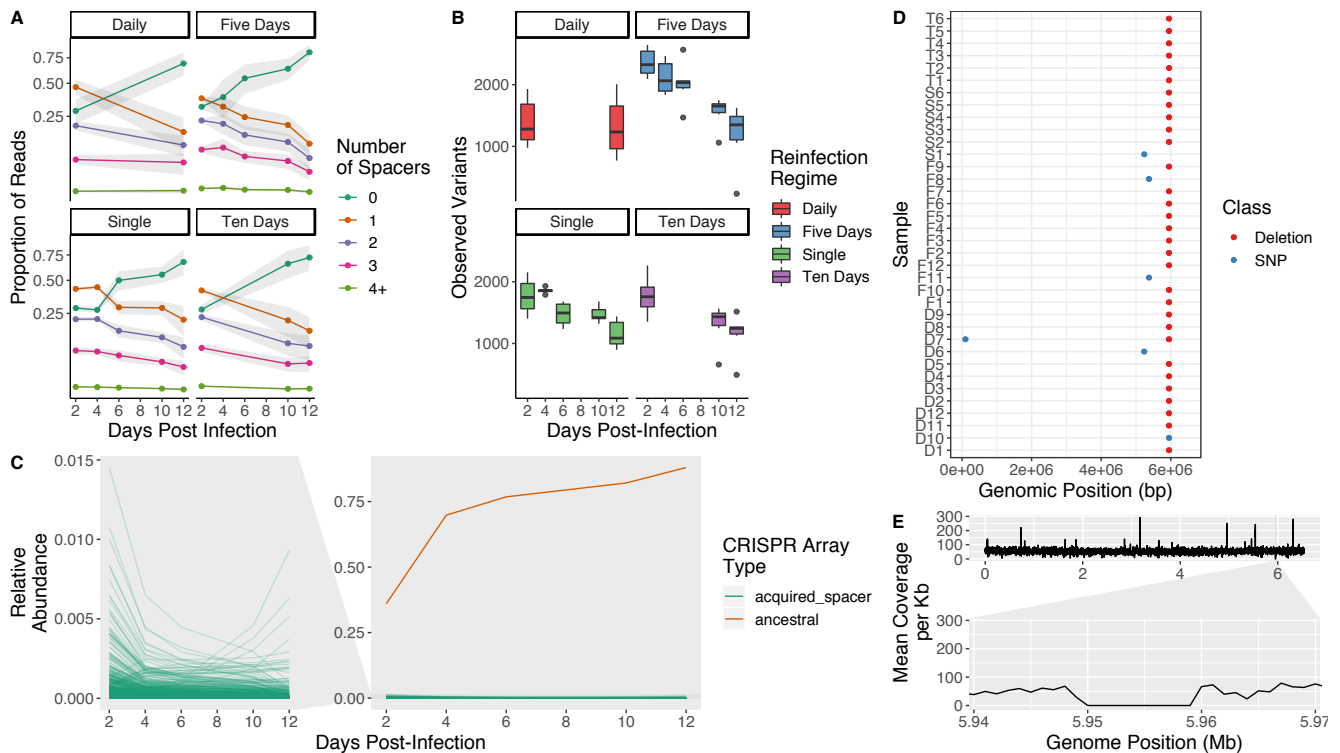
190

191 Figure 3. Population genetics of CRISPR arrays and surface mutants. A) Mean proportion of

192 reads with acquired spacers per treatment. Ribbon denotes 1 S.D. B) Decline in genetic

193 diversity in spacer arrays across treatments. These results are qualitatively similar regardless

194 of diversity index used (i.e. Shannon, Simpson's). C) Frequencies of individual arrays

195 through time for a single population of the five-day reinfection regime. Orange line

196 represents the ancestral array, with no new spacer. Green lines represent unique genotypes.

197 Zoomed panel shows individual spacer frequencies. Figures show the results for CR2, the

198 more active locus, however these results are also representative of CR1. D) Whole genome

199 analysis of re-sequenced clones exhibiting a surface modification phenotype at day 12- points

200 denote SNP locations. Sample names denote infection regime and replicate. E) Mean

201 coverage of reads across the PA14 genome, for a single sample (S2), split by 1Kb intervals.

202 Zoomed panel shows the 10,288 bp deletion containing pilus genes.

203

204 *Sensitive bacteria act as a reservoir for phage amplification*

205   The data discussed above show that CRISPR immunity dominates early on, but over time

206   sensitive bacteria and SM clones invade. Since sensitive bacteria will act as a source for

207   phage, we hypothesised that their invasion may be responsible for the observed bacteria-

208   phage coexistence following re-infections at 10 dpi. Consistent with this hypothesis, bacterial

209   populations from 2 dpi were able to rapidly reduce phage DMS3vir titres whereas the same

210   populations from 12 dpi caused phage amplification (GLM, $F_{1,46}$ = 172.29, p < 0.0001, Fig.

211   S2). Moreover, we found a strong interaction effect between phage titres and the proportion

212   of each phenotype in our experimental populations (GLM, $F_{1,627}$ = 50.93, p < 0.0001).

213   Specifically, we found a positive correlation between phage titre and the frequency of

214   sensitive clones in the population (GLM, $F_{1,209}$ = 12.3, adjusted p-value < 0.001), as well as a

215   negative correlation between phage titre and the frequency of CRISPR-immune clones

216   (GLM, $F_{1,209}$, F = 41.6, adjusted p-value < 0.001) (Fig 4.). As expected, the proportion of

217   clones with SM resistance correlates less strongly with phage titre (as this phenotype neither

218   amplifies nor degrades phages). Taken together, these results are consistent with the idea that

219   CRISPR clones act as a 'sink' for phages whilst sensitive bacteria act as a 'source' for phages

220   and that the protective effect is lost as CRISPR-immune bacteria decline in frequency.
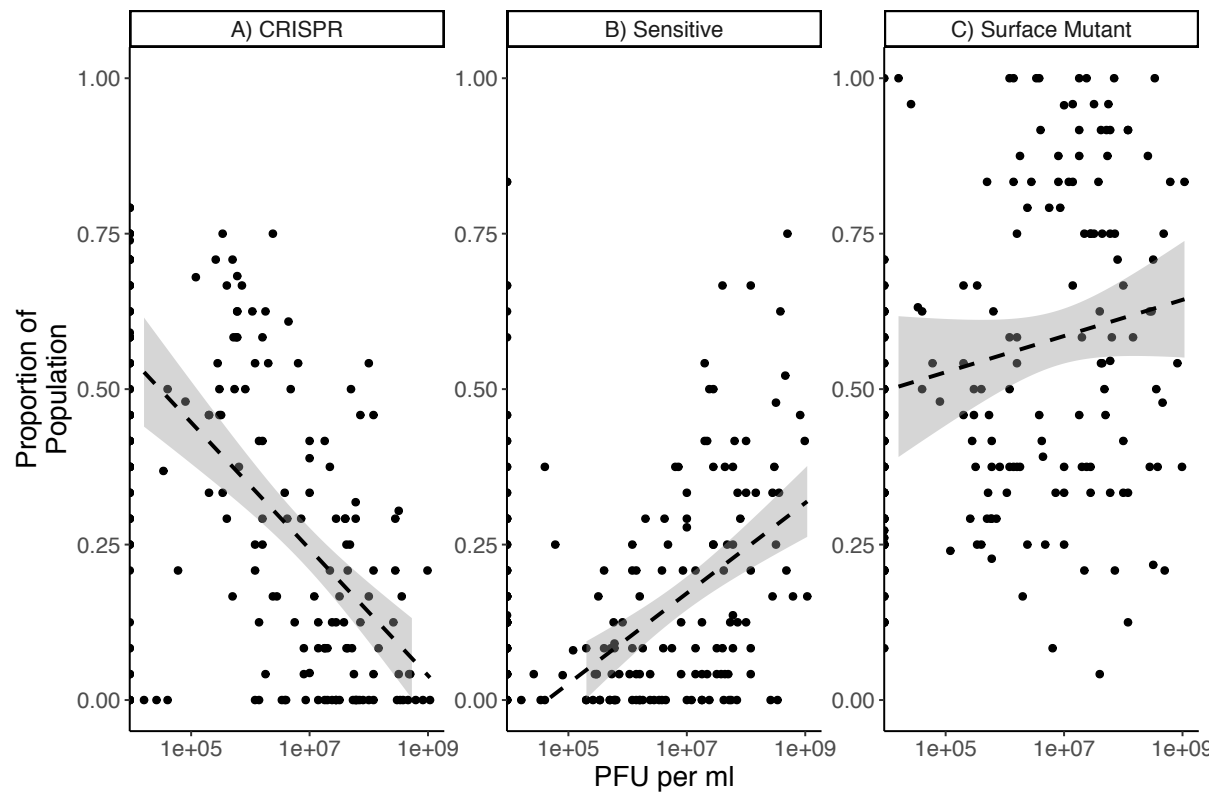
221

222

223

Figure 4. Correlations of each phenotype with phage titres throughout the experiment.

Dashed lines represent a linear model fit and shaded areas represent 95% confidence

intervals. A) Surface mutant bacteria, B) CRISPR-immune bacteria, C) Sensitive bacteria.

Phage densities drive the host evolutionary dynamics

Whereas invasion of sensitive bacteria can explain the phage population dynamics, it is less

clear what drives the invasion of sensitives in the first place. To understand this, we first

compared the host dynamics across the different infection regimes. Even though the decline

of CRISPR-immune clones was broadly similar across the various infection regimes, there

were clear differences in the invasion of sensitive bacteria and clones with SM resistance that

depended on the phage titers: sensitive bacteria were most likely to increase in frequency

when phages were absent, whereas SM tended to invade in the presence of phage (GLM,

interaction between phage presence and phenotype on change in frequency, $F_{1,611} = 30.87$, p

237   < 0.001, Fig S3). Invasion of sensitives in the absence of phage may be driven by selection,

238   if sensitive bacteria are fitter than clones with CRISPR immunity under those conditions.

239   However, the observed increase in the frequency of sensitives may also result from back-

240   mutation from a CRISPR immune genotype to sensitive (for example mutations in *cas* genes

241   can inactivate the immune system (Jiang *et al.* 2013) or recombination between CRISPR

242   repeats can result in spacer loss (Lopez-Sanchez *et al.* 2012). To tease these processes apart,

243   we competed clones with different phenotypes isolated from these evolution experiments

244   against an ancestral reference strain in the absence of phages. We found that although the

245   clones did increase in fitness by day 12 (GLMM, main effect of time, $\chi^2 = 31.07$, df = 6, p <

246   0.001, Fig. 5), there was no interaction between phenotype and time (GLMM, $\chi^2 = 3.11$, df =

247   11, p = 0.21) and no effect of treatment (GLMM, $\chi^2 = 1.83$, df = 9, p = 0.61). We also found

248   a borderline significant effect of phenotype (GLMM, $\chi^2 = 6.54$, df = 6, p = 0.038), however

249   post-hoc testing showed that there were no significant differences among phenotypes within

250   each timepoint (Table S1). When considered alongside the observed ecological dynamics, the

251   most parsimonious explanation is that sensitive bacteria invade the populations through the

252   loss of CRISPR immunity i.e. back-mutation where spacers are lost. This is most clear in the

253   single infection treatment where phages are absent: no phenotype has greater fitness yet

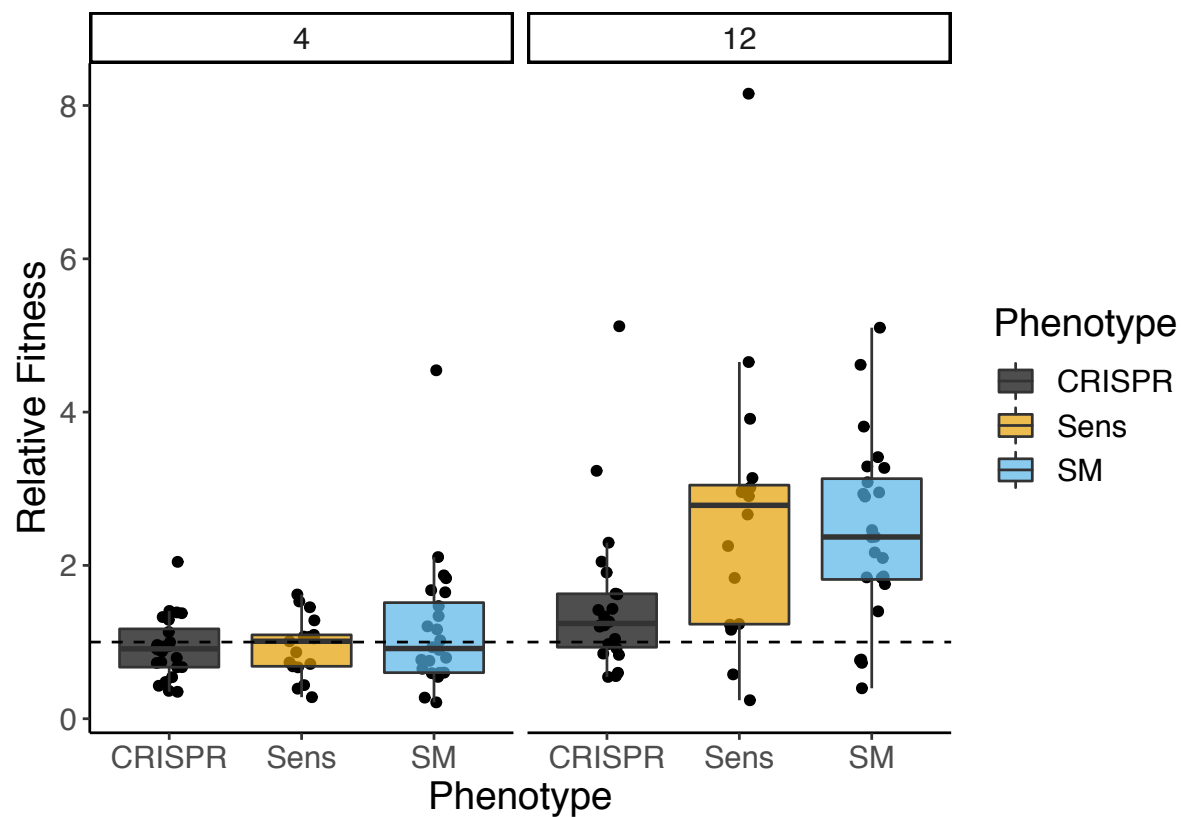254   sensitive bacteria still invade (Fig. 2).

Fig. 5. Relative fitness of bacterial clones at early (day 4) and late (day 12) timepoints during the experiment (in the absence of phages). Relative fitness was determined from 3-day competition experiments against a marked reference strain in the absence of phages. Where possible, a clone of each phenotype was isolated from all populations. A) Clones isolated from 4 DPI, B) Clones isolated from 12 DPI.

In contrast, the rapid invasion of SM clones observed in the evolution experiment, in the presence of phage, is likely explained by the fact that CRISPR immunity is associated with an inducible cost (i.e. a cost that increase during phage infections (Westra *et al.* 2015). Indeed, a similar invasion of SM has been previously observed when a reservoir of sensitive bacteria was introduced because the force of infection is increased (Chabas *et al.* 2016). However, it has remained unclear what the mechanistic basis of this cost is. We envisaged

269   three possible reasons for this inducible cost: (i) a cost of autoimmunity, where bacteria

270   acquire self-targeting spacers during infections (ii) a fitness cost due to enhanced expression

271   of the CRISPR-Cas immune system following infection or (iii) due to expression of phage-

272   encoded genes in the period between infection (i.e. phage genome injection) and CRISPR-

273   mediated clearance of the phage. To explore the first hypothesis, we first performed a

274   competition experiment between bacteria with CRISPR immunity that are unable to acquire

275   novel spacers (i.e. a *cas1* deletion mutant) and a surface mutant. This competition was

276   performed across a gradient of titres of DMS3mvir (a mutant of DMS3vir that is targeted by

277   spacer1 in CRISPR array 2 of the PA14Δ*cas1* strain; hence both the surface mutant and

278   competing bacterial genotypes being insensitive to this phage). If the induced fitness cost of

279   CRISPR-Cas immunity was due to the acquisition of self-targeting spacers, we would expect

280   the *cas1* deletion mutant to outcompete the WT strain. However, this was not observed, with

281   the *cas1* deletion mutant showing lower relative fitness than the WT strain (GLM, $F_{1,70} =$

282   17.85, p < 0.001, Fig. S4). This suggests that the observed phage-induced fitness cost is not

283   due to autoimmunity. Similarly, deep sequencing of bacterial populations that evolved phage

284   resistance against DMS3vir showed that self-targeting with either zero (n = 17) or a single

285   mismatch (n = 18) to the host-genome spacers were very rare (0.16% of all unique spacers).

286   However, one spacer was found to target both the phage and host genome with 100%

287   sequence identity (hypothetical protein YP_950448.1 and DUF1804 family protein

288   respectively). While this spacer was present in two populations, it was only observed at the

289   first timepoint sampled (day 2), consistent with the idea that there is strong selection against a

290   self-targeting spacer. Our results therefore suggest that although self-targeting is likely to be

291   deleterious, it is insufficient to explain the initial invasion of SM clones.

292   To explore whether expression of either host or phage genes following phage

293   infection caused the phage-induced cost of CRISPR-based immunity, we performed RNAseq

294   at 35, 60 and 120 minutes post-infection of a CRISPR immune clone that carries 2 spacers

295   targeting DMS3vir (BIM2). BIM2 shows complete immunity to DMS3vir and no phage

296   particles are produced following infection (data not shown; also see Landsberger *et al.* 2018).

297   Differential expression analysis found no evidence that CRISPR-Cas expression is enhanced

298   following infection (Fig. S5). Of all CRISPR-Cas genes, only Cas1 showed a significant

299   difference, with slightly lower expression in infected BIM2 populations relative to controls

300   (FDR adjusted p-value = 0.017, log2 fold change = - 0.375). Finally, to test whether we

301   could detect phage gene expression in the infected BIM2 populations we mapped reads to the

302   DMS3vir genome. This revealed significant levels of genome-wide phage gene expression in

303   the BIM2 populations, despite their CRISPR-based immunity. In total, phage expression in

304   the BIM2 populations was around 5-fold lower compared to infected WT populations (Fig.

305   S6). Amongst the expressed phage genes, we identified very high levels of anti-CRISPR

306   (*acr*) and associated repressor (*aca*) expression (Fig. S6), which has previously been reported

307   to be amongst the most strongly expressed genes on the phage DMS3vir genome (Stanley *et*

308   *al.* 2019), and to a lesser degree, many other genes (Fig S7). This *acr* protein is specific for

309   type I-E CRISPR-Cas systems and does not impact the type I-F CRISPR-Cas system encoded

310   by PA14. Collectively, these data show that the phage is capable of expressing its genes prior

311   to CRISPR mediated cleavage.

312   To test whether expression of the *acr* or *aca* genes might be responsible for the

313   phage-induced fitness cost in CRISPR-immune bacteria, we next competed the BIM2 strain

314   and the surface mutant in the presence of either WT DMS3vir, an *acr* deletion mutant, and a

315   mutant carrying a deletion of the entire *acr* operon. This revealed a similar fitness cost

316   regardless of the phage genotype (GLM, effect of genotype on relative fitness of BIM vs SM,

317     $F_{1,50} = 2.15$, p = 0.12). However, given that many other phage genes are also expressed, albeit

318   at lower levels, the induced cost may well be due to expression of one or more other phage

319   genes. We hypothesized that expression of the protease I gene might be particularly costly,

320   since proteolytic activity could conceivably cause cytotoxicity in the cell. This essential gene

321   is located immediately downstream of the *acr* and *aca* genes, and was found to be expressed

322   both in this experiment as well as an independent RNAseq experiment using nanopore

323   sequencing (data not shown). Given that a protease I deletion mutant would not be viable, we

324   cloned and expressed the protease gene in WT *P. aeruginosa* to measure the cost of

325   expression of this gene for the host. This showed that protease I expression reduced cell

326   growth rates by approximately 13% relative to an empty vector control (GLM, $F_{1,46} = 28.72$,

327    $p < 0.001$). Given that this is just one of the many genes expressed by the phage during

328   infection it seems likely that phage gene expression prior to clearance of the infection is a

329   source of the observed phage-induced cost of CRISPR-based immunity. However, we note

330   that there may be additional unknown factors that contribute to an inducible-cost.

331

332

333

334   ***Discussion***

335   Here we demonstrate that bacteria are rapidly immunised following phage infection and the

336   population is driving the phage to extinction. However, the success of this immunisation is

337   transient and successive re-introduction of the phage leads to stable coexistence between

338   bacteria and phages. This is due to the invasion of bacteria with SM resistance as well as

339   sensitive bacteria, which is caused by both an inducible fitness cost of CRISPR-based

340   immunity and the loss of spacers. We attribute the inducible cost to the phage gene

341   expression we observe which likely occurs prior to clearance of the infection by the CRISPR

342   immune system. Immune loss has been shown to result in the stable coexistence of bacteria

343   and phages (Weissman *et al* 2018.; Chaudhry *et al.* 2018) and the loss of spacers, resulting in

344   a loss of immunity, is highly consistent the ecological dynamics we observe.

345

346   In a broader context, parasites are often invoked as a selective force for maintaining host

347   diversity through negative frequency dependent selection (Koskella & Lively 2009).

348   However, the effectiveness of CRISPR-Cas in driving phage extinct shortly after the onset of

349   the phage epidemic (van Houte *et al.* 2016), removes this key mechanism for maintaining

350   host spacer diversity. Indeed, we observed that spacer diversity decreased in all treatments

351   (Fig. 3). This rapid decline in CRISPR diversity also helps to explain the observed

352   conservation of the trailer-end of CRISPR loci (Tyson & Banfield 2007), although other

353   ecological and evolutionary processes, such as selective sweeps of multi-phage resistant

354   CRISPR clones (Weinberger *et al.* 2012), will also be important in natural communities.

355   Interestingly, we find that surface modifications that confer phage resistance in this

356   environment are not associated with a measurable trade-off in competitive fitness in the

357   absence of phage. Although the variation in the genetic basis of the SM phenotype (SNPs and

358   large deletions) suggests these mutations may vary in their fitness consequences in more

359   complex environments. For example, increasing the environmental complexity, in the form of

360   additional competitor species has been shown to amplify the associated fitness trade-off

361   (Alseth *et al.* 2019). Therefore, understanding these dynamics across a range of environments

362   will be of importance for future work.

363

364   The loss of spacer diversity over time is particularly relevant in the context of phage therapy,

365   which is experiencing renewed clinical interest (Dedrick *et al.* 2019). Long-lasting resistance

366   mechanisms may severely hamper therapeutic usage of phages, however this work shows that

367   one can take advantage of the loss of population-level CRISPR immunity over time and

368   design well-timed re-infection schemes. Clinical trials where burn wound patients are treated

369   with cocktails of *Escherichia coli* and *P. aeruginosa* phages are ongoing (Rose *et al.* 2014)

370   and experiments with murine models have demonstrated that phage therapy can provide

371   highly effective treatment of *P. aeruginosa* infections (Waters *et al.* 2017; Wright *et al.* 2009;

372   Kingwell 2015; Roach *et al.* 2017). This work also highlights an important potential issue

373   associated with long-term information storage in CRISPR loci of bacterial populations

374   (Shipman *et al.* 2017*;* Shipman *et al.* 2016), since unique spacer sequences will inevitably be

375   lost over time.

376

377   ***Materials and Methods***

378   **Bacterial strains and phages**

379   The previously described *P. aeruginosa* strains UCBPP-PA14 and the isogenic mutant

380   *csy3::LacZ* and phage DMS3vir have been previously described (Cady *et al.* 2012) and were

381   used throughout this study.

382

383   **Evolution experiments**

384   Evolution experiments were performed in 6 replicates by inoculating 6 ml M9 supplemented

385   with 0.2% glucose or LB with approximately 10^6 bacteria from fresh overnight cultures of the

386   WT strain and adding 10^7 pfu of DMS3vir, followed by incubation at 37 ºC while shaking at

387   180 rpm. Cultures were transferred daily 1:100 for 30 days. Reinfections with ancestral phage

388   (10^7 pfu) were performed as follows: a) bacterial cultures in the single infection treatment

389   were only infected at t=0 b) bacterial cultures in the 5 day re-infection treatment were

390   infected at t=0, 5, 10, 15, 20 and 25 dpi c) bacterial cultures in the 10 day re-infection

391   treatment were infected at t=0, 10 and 20 dpi d) bacterial cultures in the daily infection

392   treatment were infected at each daily transfer.

393

Phage extraction and titration

395   Every second transfer, samples were taken just before transferring of the cultures into fresh

396   medium. Phage was isolated from these samples using chloroform extractions. Next, phage

397   was titrated by spotting serial dilutions of phage in M9 salts on a lawn of *P. aeruginosa* strain

398   UCBPP-PA14 *csy3::LacZ* bacteria for quantification.

399

Deep sequencing analysis

401   Full bacterial genomic DNA was isolated using the Qiagen QIAmp DNA mini kit as per the

402   manufacturer's protocols. A PCR amplification was performed for both CRISPR arrays

403   (CRISPR1 and CRISPR2, see table S2). PCR reactions contained 5 µl DreamTaq master mix

404   (ThermoScientific, UK), 0.5 µl forward primer, 0.5 µl reverse primer, 1.5 µl MiliQ water, 0.5

405   µl DMSO, 2 µl template DNA. Sample purity was determined by NanoDrop and DNA

406   concentrations were quantified done using a Qubit fluorometer (ThermoFisher, UK).

407

CRISPR array sequencing protocol

409   Two separate CRISPR primer (CRISPR1 and CRISPR2 locus) pairs were designed for two

410   first round PCRs. 2 µl of DNA entered a first-round of PCR. The primer design incorporates

411   a recognition sequence to allow a secondary nested PCR process. Samples were first purified

412   with Ampure SPRI Beads before entering the second PCR performed to incorporate Illumina

413   adapter sequences. Samples were purified using Ampure SPRI Beads before being quantified

414   using Qubit and assessed using the Fragment Analyzer. Successfully generated amplicon

415   libraries were taken forward and pooled in equimolar amounts, then size selected on a Pippin

416   prep using a range of 180-600bps. The quantity and quality of each pool was assessed by

417   Bioanalyzer and subsequently by qPCR using the Illumina Library Quantification Kit from

418   Kapa on a Roche Light Cycler LC480II according to manufacturer's instructions. Template

419   DNA was denatured according to the protocol described in the Illumina cBot User guide and

420   loaded at 12.5 pM concentration. To help balance the complexity of the amplicon library

421   15% PhiX was spiked in. The sequencing of each pool was carried out on one lane of an

422   Illumina MiSeq, at 2x250 bp paired-end sequencing with v2 chemistry.

423

424   **Bioinformatics analysis**

425   *Sequence Quality Control*

426   Base-calling and de-multiplexing of indexed reads was performed by CASAVA version 1.8.2

427   (Illumina) to produce 97 samples from each of the 2 lanes of sequence data. FASTQ files

428   were trimmed to remove Illumina adapter sequences using Cutadapt version 1.2.1 (Martin

429   2011). The option "-O 3" was set, so the 3' end of any reads which matched the adapter

430   sequence over at least 3 bp was trimmed off. The reads were further trimmed to remove low

431   quality bases, using Sickle version 1.200 with a minimum window quality score of 20. After

432   trimming, reads shorter than 10 bp were removed. The raw reads were subjected to a

433   Cutadapt trimming step to remove PCR primer sequences that could potentially introduce an

434   artificial level of complexity in the samples. To improve base quality in both read pairs,

435   sequencing errors were corrected in both forward and reverse reads using the error-correct

436   module within SPAdes sequence assembler, version 3.1.0 (Bankevich *et al.* 2012). Read pairs

437   were aligned to produce a single sequence for each pair that would entirely span the amplicon

438   using PEAR (version 0.9.10; (Zhang *et al.* 2014)). Additionally, sequences with uncalled

439   bases (Ns) were removed. To remove sequences originating from potential PCR primer

440   dimers or from any spurious amplification events, a size selection was applied to each

441   merged sequence set, respectively between 30-140bp for CRISPR1 and 70-500bp for

442   CRISPR2. Fragmented PhiX phage genome was added to the sequence library in order to

443   increase the sequence complexity. To remove any 'bleed through' of PhiX sequences, each

444   sample was compared with the complete PhiX sequence (GenBank gi9626372) using

445   BLASTN (Altschul *et al.* 1990). Sequences matching PhiX (E-value < 10-5) were filtered out

446   of the dataset.

447

448   *Clustering and diversity metrics*

449   For each dataset, any sequences passing the filters (from any sample) were merged into a

450   single file. This final sequence file, plus its own metadata file describing each sample, was

451   used for the analysis by using a custom pipeline based on QIIME 1.9.0 (Caporaso *et al.*

452   2010). Clusters were defined using SWARM (Mahé *et al.* 2014), using the strictest (default)

453   parameters. This tool aggregates a sequence to a cluster if the sequence shows similarity with

454   any of the sequences already present in that cluster. Importantly, the similarity threshold is

455   not fixed but defined within the dataset. A minimum cluster size filter is applied to retain

456   clusters containing at least 2 sequences and potential chimeric-sequences due to PCR events

457   were discarded as well. To calculate the abundance of each cluster, sequences were then

458   aligned on the centroid sequence identified for each clusters, using a minimum similarity

459   threshold of 99% for the entire length of the sequence using the 'usearch_global' function in

460   VSEARCH.

461

462   The sequencing depth of all samples was explored using the 'Chao 1' (Chao, 1984) richness

463   index plotted as a rarefaction curve. Counts in the cluster abundance tables were repeatedly

464   sub-sampled (rarefied; 33 repetitions) at sampling depths of 1000, 12000, 22000, … 150000.

465   The average Chao1 value obtained by repeating the test 33 times is assigned as alpha-

466   diversity at that specific number of reads for that sample implemented in Qiime. Because all

467   samples reached a clear asymptote, i.e. no samples were under-sampled with regards to

468   spacer diversity, rarefaction was not applied. An abundance table for each locus was used to

469   estimate the richness and evenness of the samples using the following estimators: total

470   observed sequence variants, Shannon, Simpson, Simpson evenness again conducted with

471   Qiime.

472

473   *Whole-genome sequencing*

474

475   Populations from T12 were plated and 12 resulting colonies were screened for their phage

476   resistance phenotype, as described above. An additional control of the ancestral PA14

477   laboratory stock was included. Each colony was then suspended in 100 ul H_2O and streaked

478   across an LB agar plate. Cells were scraped from these plates and added to bead beating tubes

479   prior to shipping to the MicrobesNG service (Birmingham UK). Three beads were washed

480   with extraction buffer containing lysozyme and RNase A, incubated for 25 min at 37 C.

481   Proteinase K and RNaseA were added and incubated for 5 min at 65 C. Genomic DNA was

482   purified using an equal volume of SPRI beads and resuspended in EB buffer. DNA was

483   quantified in triplicates with the Quantit dsDNA HS assay in an Ependorff AF2200 plate

484   reader. Genomic DNA libraries were prepared using Nextera XT Library Prep Kit (Illumina,

485   San Diego, USA) following the manufacturer's protocol with the following modifications:

486   two nanograms of DNA instead of one were used as input, and PCR elongation time was

487   increased to 1 min from 30 seconds. DNA quantification and library preparation were carried

488   out on a Hamilton Microlab STAR automated liquid handling system. Pooled libraries were

489   quantified using the Kapa Biosystems Library Quantification Kit for Illumina on a Roche

490   light cycler 96 qPCR machine. Libraries were sequenced on the Illumina HiSeq using a

491   250bp paired end protocol. Reads were adapter trimmed using Trimmomatic 0.30 with a

492   sliding window quality cutoff of Q15 (Bolger *et al.* 2014). The ancestral control was initially

493   mapped to the PA14 reference genome (NC_008463) using the Breseq pipeline (version

494   0.32.0, (Deatherage & Barrick 2014). The reference genome was then modified to match the

495   identified mutations (to account for divergence between the laboratory strain and original

496   reference genome). The remaining samples were then mapped against this modified reference

497   and alignments were used for identifying mutations.

498

499

500   **Immunity and resistance profiling**

501   Bacterial immunity against the ancestral phage was determined as described before (Westra

502   *et al.* 2015; van Houte *et al.* 2016; Chabas *et al.* 2018) by streaking individual clones (24

503   clones per sample) through ancestral phage DMS3vir and phage DMS3vir carrying the anti-

504   CRISPR F1 (*acrIF1*) gene (Bondy-Denomy *et al.* 2012). Bacterial clones sensitive to both

505   phages were scored as "sensitive", those resistant to DMS3vir but sensitive to

506   DMS3vir+AcrF1 were scored as "CRISPR immune", and bacterial clones resistant to both

507   phages were scored as "surface mutants". CRISPR-Cas-mediated immunity was further

508   confirmed by PCR using primers CTAAGCCTTGTACGAAGTCTC and

509   CGCCGAAGGCCAGCGCGCCGGTG (for CRISPR 1) and

510   GCCGTCCAGAAGTCACCACCCG and TCAGCAAGTTACGAGACCTCG (for CRISPR

511   2). Surface modification was further confirmed on the basis of colony morphology (since

512   phage DMS3vir is pilus-specific, surface mutants have motility defects, resulting in a

513   modified colony morphology) and a lack of new CRISPR spacers. From these analyses

514   fractions of each phenotype (sensitive, CRISPR immune, surface mutant) were calculated for

515   each replicate experiment.

516

517   **Statistical analyses**

518   In most cases general linear models were used using the appropriate error structure and

519   model residuals were assessed for model fit. Significance was determined following stepwise

520   deletion of terms or through Tukey post-hoc testing with adjustment for multiple

521   comparisons. General linear mixed-effect models were used for the competition assays, with

522   population specified as a random effect, due to the non-independence of clones isolated from

523   the same populations. Mixed effect modelling was carried out using the 'lme4' package with

524   post-hoc testing conducted with the 'emmeans' package. For gene expression analysis, data

525   were analysed with the DESeq2 pipeline using a parametric fit for the dispersion (Love *et al.*

526   2014). Statistical analyses were carried out in Rstudio using R version 3.5.2.

527

528   **Gene expression profiling**

529   Ten replicate cultures of PA14 BIM2 and 5 of WT were grown in microcosms of 6 mL LB

530   media and standardized to an optical density of 0.5 OD600 (approx. 2 X 10^9 CFU / mL).

531   Five cultures of BIM2 and 5 cultures of WT were inoculated with 8 X 10^9 PFU (in 500 uL)

532   DMS3vir (MOI 0.5) and 5 cultures of BIM2 remained uninoculated as controls. After 35

533   minutes, 1 hour and 2 hours, 1.5 mL of cells were pelleted and snap-frozen at – 80 C. For

534   RNA extraction, 1 mL of TRIzol reagent was added immediately after removal from freezer.

535   BCP was used as a phase separator followed by PureLink RNA extraction (Invitrogen) that

536   included a DNAse treatment step. Sample quantities, purities and size distribution were

537   quantifed by Qubit, nanodrop and TapeStation respectively. 150bp libraries were prepared

538   with the TruSeq directional kit and sequenced on an Illumina NovaSeq at Exeter University

539   sequencing centre.

540

541   The resulting reads were quality filtered using Sickle (default settings, version 1.33) with

542   approx. 6 million read pairs per sample remaining. These were subsequently mapped to the

543   PA14 and DMS3vir reference genomes with bwa (default settings, version 0.7.17). The

544   resulting read alignments were assigned to genomic features and counted using HTSeq

545   (version 0.11.2, (Anders *et al.* 2015) using 'union' mode, non-unique setting set to 'none'

546   and the reverse stranded option. Differential expression analysis was conducted in R using

547   the DESeq2 package (Love *et al.* 2014).

548

549   **ProteaseI expression**

550   The proteaseI gene from DMS3vir was cloned into the pHERD30T vector under control of an

551   arabinose inducible promoter. Primers used for cloning are available in table S3. Colonies

552   were selected using a gentamycin marker and blue/white colony screening in a background of

553   dH5-alpha cells (New England Biolabs, UK). The resulting construct was transformed into

554   PA14 and the clone used for assays was verified by Sanger sequencing (University of

555   Sheffield, UK). Optical density was recorded during a 24-hour growth curve at 37 C in LB

556   supplemented with 1% arabinose. Growth curves of the clone expressing proteaseI and an

557   empty vector control were recorded. Growth rate during log-phase was extracted from the

558   growth curves in R (version 3.5.2).

559

560   **Competition assays**

561   For each population, a single clone of each phenotype (CRISPR, SM, Sens.) was picked

562   (where possible) and competed against a LacZ marked reference strain. Populations were

563   serially transferred with a 1:100 dilution in M9 media supplemented with 0.2% glucose.

564   Populations were plated at T = 0 and after 3 days on LB agar supplemeted with 30 μg of X-

565   gal to determine the relative frequencies of the clone and the reference. Selection coefficients

566   were determined as described in (van Houte *et al.* 2016).

567
568   *Data availability*
569

570   Sequence data is available from the European Nucleotide Archive under study number

571   PRJEB31514.

572   ***Author contributions***

573   E.R.W., S.v.H., S.M. and A.B. designed experiments. L.C. and S.M. performed the

574   experiments under supervision of S.v.H. and E.R.W. E.O. prepared samples for sequencing.

575   S.M., L.L., A.Biswas. performed sequencing data analyses. E.R.W. and S.M. wrote the

576   manuscript.

577

578   ***Acknowledgements***

587

588   References

589   Alseth EO, Pursey E, Luján AM *et al.* (2019) Bacterial biodiversity drives the evolution of

590   CRISPR-based phage resistance. *Nature*, **574**, 549–552.

591   Altschul SF, Gish W, Miller W *et al.* (1990) Basic local alignment search tool. *Journal of*

592   *Molecular Biology*, **215**, 403–410.

593   Anders S, Pyl PT, Huber W (2015) HTSeq--a Python framework to work with high-

594   throughput sequencing data. *Bioinformatics*, **31**, 166–169.

595   Balogh B, Jones JB, Iriarte FB, Momol MT (2010) Phage therapy for plant disease control.

596   *Current pharmaceutical biotechnology*, **11**, 48–57.

597   Bankevich A, Nurk S, Antipov D *et al.* (2012) SPAdes: a new genome assembly algorithm

598   and its applications to single-cell sequencing. *Journal of computational biology*, **19**,

599   455–77.

600   Bolger AM, Lohse M, Usadel B (2014) Trimmomatic: a flexible trimmer for Illumina

601   sequence data. *Bioinformatics*, **30**, 2114–2120.

602   Bondy-Denomy J, Pawluk A, Maxwell KL, Davidson AR (2012) Bacteriophage genes that

603   inactivate the CRISPR/Cas bacterial immune system. *Nature*, **493**, 429–432.

604   Budzik JM, Rosche WA, Rietsch A, O'Toole GA (2004) Isolation and characterization of a

605   generalized transducing phage for Pseudomonas aeruginosa strains PAO1 and PA14.

606   *Journal of bacteriology*, **186**, 3270–3.

607   Cady KC, Bondy-Denomy J, Heussler GE, Davidson AR, O'Toole, GA (2012) The

608   CRISPR/Cas adaptive immune system of Pseudomonas aeruginosa mediates resistance

609   to naturally occurring and engineered phages. *Am Soc Microbiol*. **194**, 5728-5738.

610   Canchaya C, Fournous G, Chibani-Chennoufi S, Dillmann M-L, Brüssow H (2003) Phage as

611   agents of lateral gene transfer. *Current Opinion in Microbiology*, **6**, 417–424.

612   Caporaso JG, Kuczynski J, Stombaugh J *et al.* (2010) QIIME allows analysis of high-

613   throughput community sequencing data. *Nature methods*, **7**, 335–6.

614   Chabas H, van Houte S, Høyland-Kroghsbo NM, Buckling A, Westra ER (2016)

615   Immigration of susceptible hosts triggers the evolution of alternative parasite defence

616   strategies. *Proceedings of the Royal Society B: Biological Sciences*, **283**, 20160721.

617   Chabas H, Lion S, Nicot A *et al.* (2018) Evolutionary emergence of infectious diseases in

618   heterogeneous host populations. *PLoS biology*, **16**, e2006738.

619   Chaudhry WN, Pleška M, Shah NN *et al.* (2018) Leaky resistance and the conditions for the

620   existence of lytic bacteriophage. *PLOS Biology*, **16**, e2005971.

621   Common J, Morley D, Westra ER, van Houte S (2019) CRISPR-Cas immunity leads to a

622   coevolutionary arms race between *Streptococcus thermophilus* and lytic phage.

623   *Philosophical Transactions of the Royal Society B: Biological Sciences*, **374**, 20180098.

624   Dalcin Martins P, Danczak RE, Roux S *et al.* (2018) Viral and metabolic controls on high

625   rates of microbial sulfur and carbon cycling in wetland ecosystems. *Microbiome*, **6**, 138.

626   Daly RA, Roux S, Borton MA *et al.* (2019) Viruses control dominant bacteria colonizing the

627   terrestrial deep biosphere after hydraulic fracturing. *Nature Microbiology*, **4**, 352–361.

628   Deatherage DE, Barrick JE (2014) Identification of mutations in laboratory-evolved microbes

629   from next-generation sequencing data using breseq. *Methods in Molecular Biology*,

630   **1151**, 165–188.

631   Dedrick RM, Guerrero-Bustamante CA, Garlena RA *et al.* (2019) Engineered bacteriophages

632   for treatment of a patient with a disseminated drug-resistant Mycobacterium abscessus.

633   *Nature Medicine*, **25**, 730–733.

634   Gurney J, Pleška M, Levin BR (2019) Why put up with immunity when there is resistance:

635   an excursion into the population and evolutionary dynamics of restriction–modification

636   and CRISPR-Cas. *Philosophical Transactions of the Royal Society B: Biological*

637   *Sciences*, **374**, 20180096.

638   van Houte S, Ekroth AKE, Broniewski JM *et al.* (2016) The diversity-generating benefits of a

639   prokaryotic adaptive immune system. *Nature*, **532**, 385–388.

640   Jiang, W, Maniv, I, Arain, F, Wang, Y, Levin, BR, & Marraffini, LA (2013). Dealing with

641   the evolutionary downside of CRISPR immunity: bacteria and beneficial plasmids. *PLoS*

642   *genetics*, **9**, e1003844.

643   Kingwell K (2015) Bacteriophage therapies re-enter clinical trials. *Nat Rev Drug Discov*, **14**,

644   515-516.

645   Koskella B, Brockhurst MA (2014) Bacteria-phage coevolution as a driver of ecological and

646   evolutionary processes in microbial communities. *FEMS microbiology reviews*, **38**,

647   916–31.

648   Koskella B, Lively CM (2009) Evidence for negative frequency-dependent selection during

649   experimenal coevolution of a freshwater snail and a sterilizing trematode. *Evolution*, **63**,

650   2213–2221.

651   Kutter E, De Vos D, Gvasalia G *et al.* (2010) Phage Therapy in Clinical Practice: Treatment

652   of Human Infections. *Current Pharmaceutical Biotechnology*, **11**, 69–86.

653   Labrie SJ, Samson JE, Moineau S (2010) Bacteriophage resistance mechanisms. *Nature*

654   *reviews. Microbiology*, **8**, 317–27.

655   Lopez-Sanchez, MJ, Sauvage, E, Da Cunha, V, Clermont, D, Ratsima Hariniaina, E,

656   Gonzalez-Zorn, B, Poyart, C, Rosinski-Chupin, I and Glaser, P (2012) The highly dynamic

657   CRISPR1 system of Streptococcus agalactiae controls the diversity of its

658   mobilome. *Molecular microbiology*, **85**, 1057-1071.

659   Love MI, Huber W, Anders S (2014) Moderated estimation of fold change and dispersion for

660   RNA-seq data with DESeq2. *Genome Biology*, **15**, 550.

661   Mahé F, Rognes T, Quince C et al. (2015) Swarm v2: highly-scalable and high-resolution

662   amplicon clustering. *PeerJ*, **3**, e1420.

663   Marraffini LA (2015) CRISPR-Cas immunity in prokaryotes. *Nature*, **526**, 55–61.

664   Martin M (2011) Cutadapt removes adapter sequences from high-throughput sequencing

665   reads. *EMBnet.journal*, **17**, 10-12.

666   Paez-Espino D, Morovic W, Sun CL *et al.* (2013) Strong bias in the bacterial CRISPR

667   elements that confer immunity to phage. *Nature Communications*, **4**, 1430.

668   Paterson S, Vogwill T, Buckling A *et al.* (2010) Antagonistic coevolution accelerates

669   molecular evolution. *Nature*, **464**, 275–278.

670   Roach DR, Leung CY, Henry M *et al.* (2017) Synergy between the Host Immune System and

671   Bacteriophage Is Essential for Successful Phage Therapy against an Acute Respiratory

672   Pathogen. *Cell Host & Microbe*, **22**, 38-47.e4.

673   Rose T, Verbeken G, Vos D De *et al.* (2014) Experimental phage therapy of burn wound

674   infection: difficult first steps. *International Journal of Burns and Trauma*, **4**, 66.

675   Shipman S, Nivala J, Macklis J, *et al.* (2017) CRISPR–Cas encoding of a digital movie into

676   the genomes of a population of living bacteria. *Nature*, **547**, 345.

677   Shipman S, Nivala J, Macklis J, *et al.* (2016) Molecular recordings by directed CRISPR

678   spacer acquisition. *Science*, **353**, aaf1175.

679   Stanley SY, Borges AL, Chen K-H *et al.* (2019) Anti-CRISPR-Associated Proteins Are

680   Crucial Repressors of Anti-CRISPR Transcription. *Cell*, **178**, 1452-1464.e13.

681   Chao A. (1984) Nonparametric estimation of the number of classes in a population.

682   *Scandinavian Journal of statistics*, 265-270.

683   Suttle CA (2007) Marine viruses — major players in the global ecosystem. *Nature Reviews*

684   *Microbiology*, **5**, 801–812.

685   Tyson GW, Banfield JF (2007) Rapidly evolving CRISPRs implicated in acquired resistance

686   of microorganisms to viruses. *Environmental Microbiology*, **10**, 200-207.

687   Wagenaar JA, Bergen MAP Van, Mueller MA, Wassenaar TM, Carlton RM (2005) Phage

688   therapy reduces Campylobacter jejuni colonization in broilers. *Veterinary Microbiology*,

689   **109**, 275–283.

690   Waters E, Neill D, Kaman B *et al.* Phage therapy is highly effective against chronic lung

691   infections with Pseudomonas aeruginosa. *Thorax*, **72**, 666-667.

692   Weinberger AD, Sun CL, Pluciński MM *et al.* (2012) Persisting Viral Sequences Shape

693   Microbial CRISPR-based Immunity. *PLoS Computational Biology*, **8**, e1002475.

694   Weissman J, Holmes R, Barrangou R *et al.* (2018) Immune loss as a driver of coexistence

695   during host-phage coevolution. *The ISME journal*, **12**, 585.

696   Westra ER, van Houte S, Oyesiku-Blakemore S *et al.* (2015) Parasite Exposure Drives

697   Selective Evolution of Constitutive versus Inducible Defense. *Current biology*, **25**,

698   1043–1049.

699   Wright A, Hawkins CH, Anggård EE, Harper DR (2009) A controlled clinical trial of a

700   therapeutic bacteriophage preparation in chronic otitis due to antibiotic-resistant

701   Pseudomonas aeruginosa; a preliminary report of efficacy. *Clinical otolaryngology*, **34**,

702   349–57.

703   Zhang J, Kobert K, Flouri T, Stamatakis A (2013) PEAR: a fast and accurate Illumina Paired-

704   End reAd mergeR. Bioinformatics, **30**, 614-620.

705

706

707

708   **Supplementary Information**
709
710
711
712
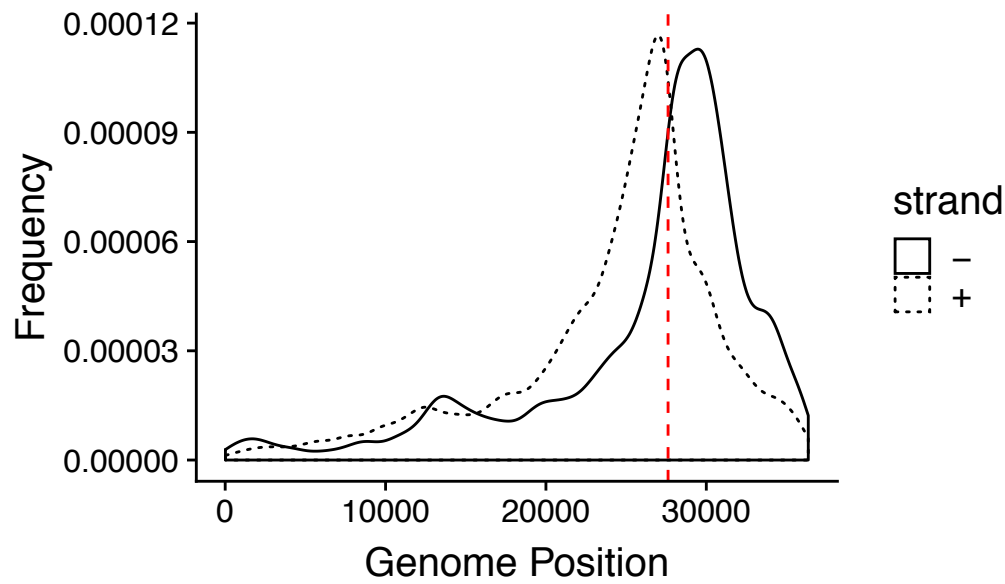
713

714   Figure S1.

715   Locations of extracted spacers from the CRISPR arrays when mapped to the DMS3vir

716   genome. Red line denotes the location of the priming spacer (CRISPR2 spacer 1).
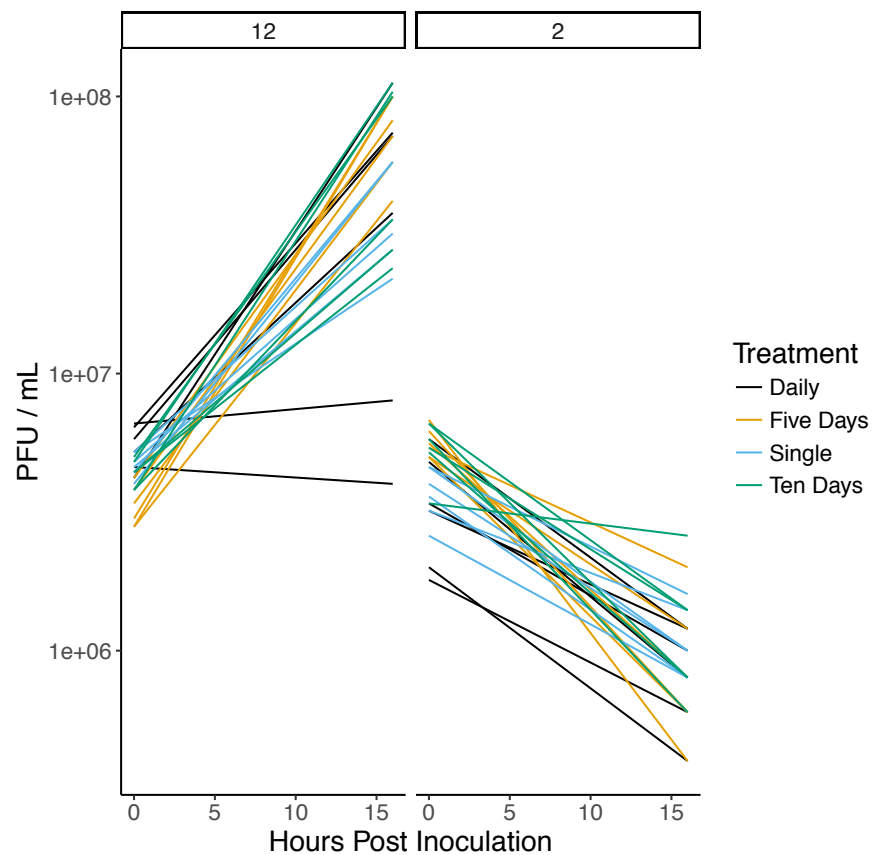
717

718

719

720

721   Figure S2.

722   Changes in phage titres upon infection with 10^7 PFU DMS3vir of populations isolated from

723   day 12 (left panel, n = 24) or day 2 (right panel, n = 24) from each of the different reinfection

724   regimes. Colours denote the reinfection regimes where the bacterial populations were derived

725   from: bacterial populations isolated from the single infection regime are shown in blue, those

726   from re-infection every five days are shown in yellow, reinfection every 10 days in green,

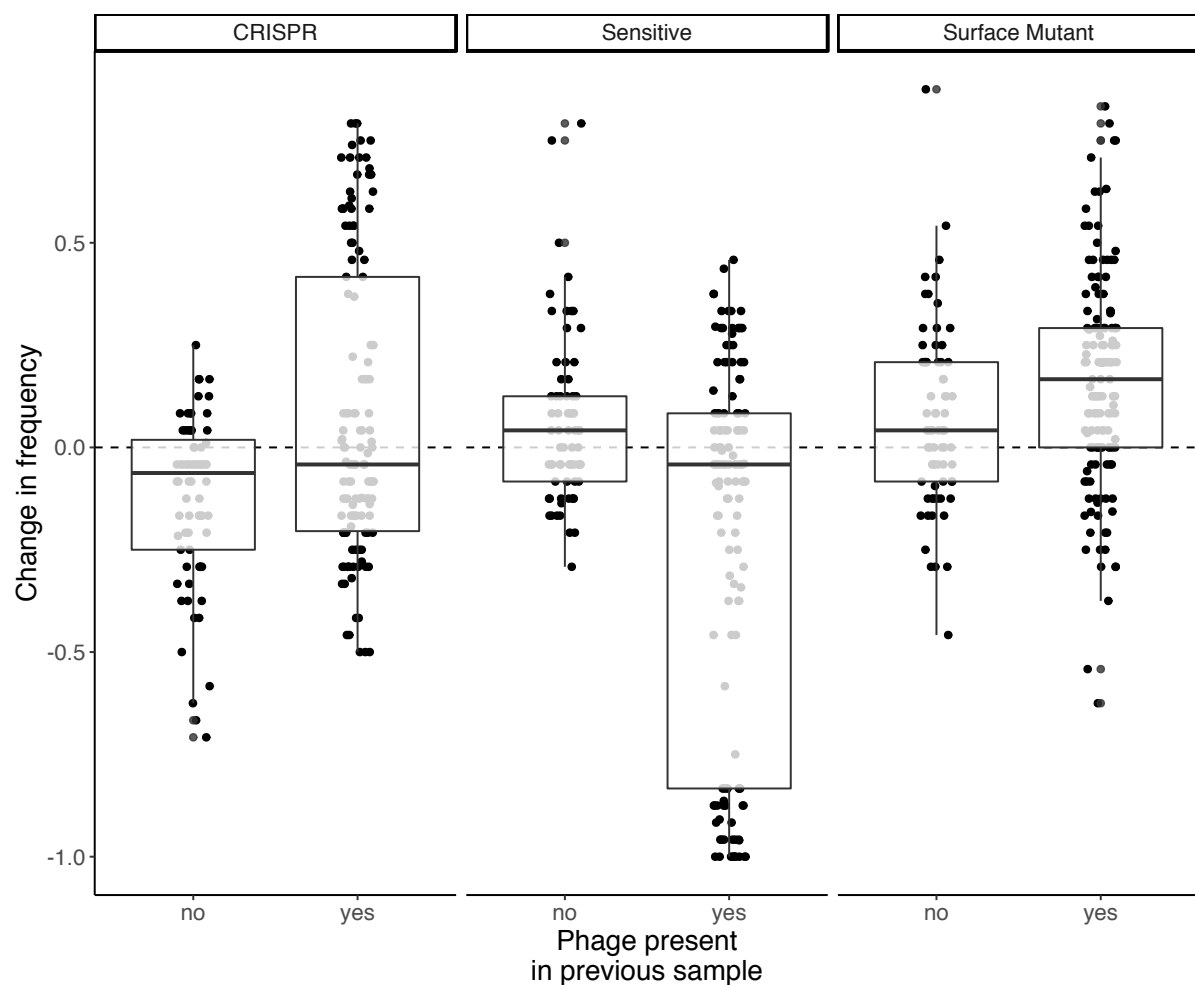727   and daily infection in black.

728

729

730

731   Fig. S3. Change in frequency of each phenotype between sampling points during evolution

732   experiment split by presence (n = 402) or absence (n = 215) of phage in the previous sample.

733   Limit of detection for phage presence is 200 PFU per ml. Boxplots show the median,

734   interquartile range and minimum and maximum values.

735

736

737
738
739

740

741
742   Figure S4.

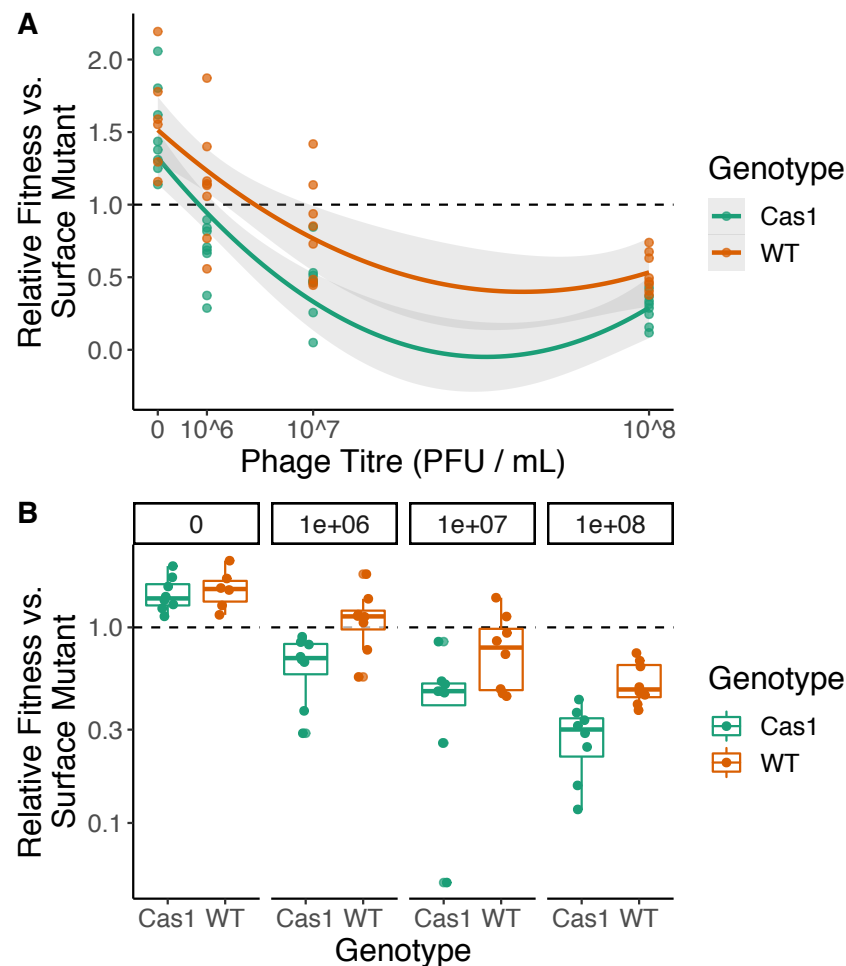743   Relative fitness of bacterial populations with CRISPR-mediated immunity at 3 d.p.i. when

744   competing with a surface mutant. Competitions were carried out between a marked surface

745   resistant strain and either the WT PA14 (purple), a mutant PA14 lacking a functional *cas1*

746   (orange) or a WT-derived strain carrying 2 additional spacers targeting phage DMS3mvir

747   (BIM2; green). Experiments were carried out across a gradient of phage titres, as indicated.

748   The phage used (DMS3mvir) is a mutant of DMS3vir that is targeted by WT PA14. N = 8

749   replicates per genotype per phage titre. A) Data presented with phage titre as a continuous

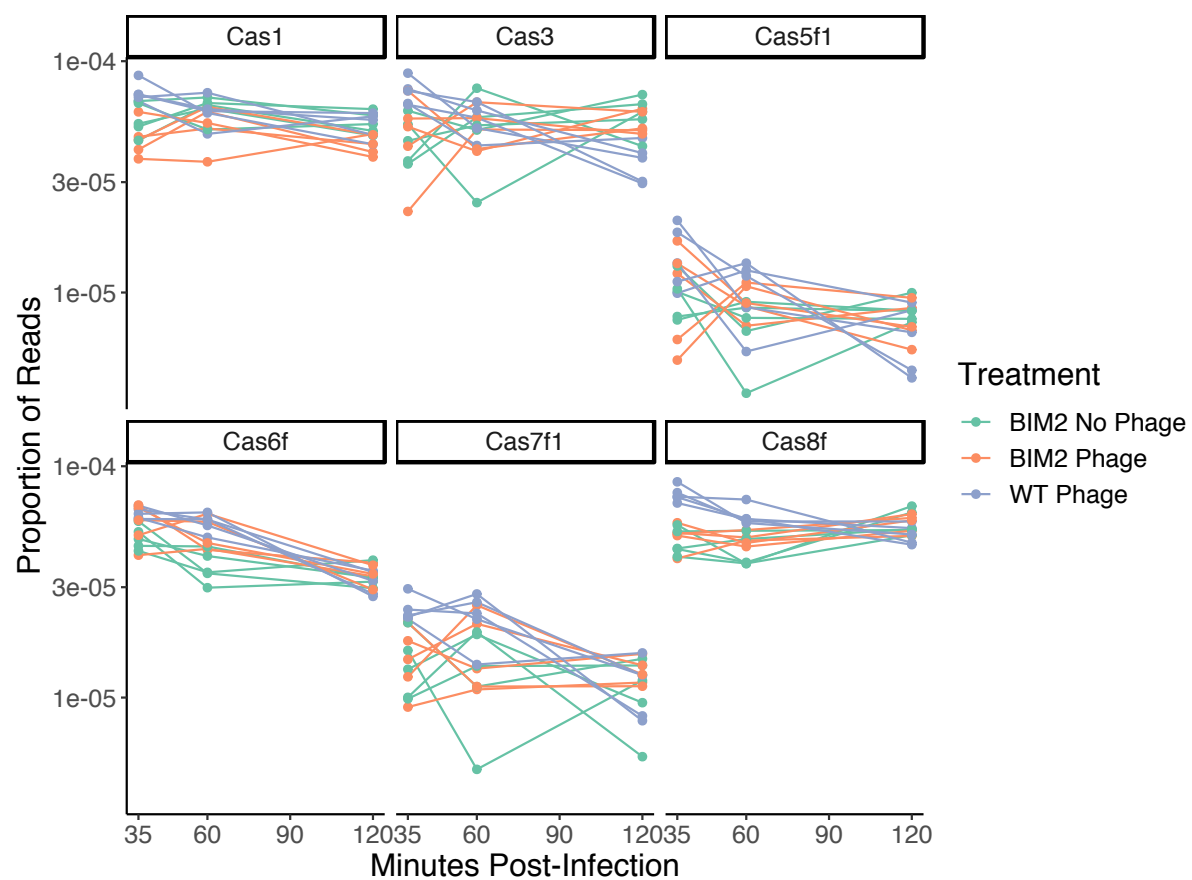750   variable. B) Data grouped by phage titre to better visualise differences within titres.

751

752

753
754   Fig. S5

755   Expression of CRISPR associated genes following infection with 8 X 10^9 PFU DMS3vir

756   (MOI 0.5) across PA14 WT (purple, n = 5), PA14 BIM2 (orange, n = 5) and PA14 BIM2

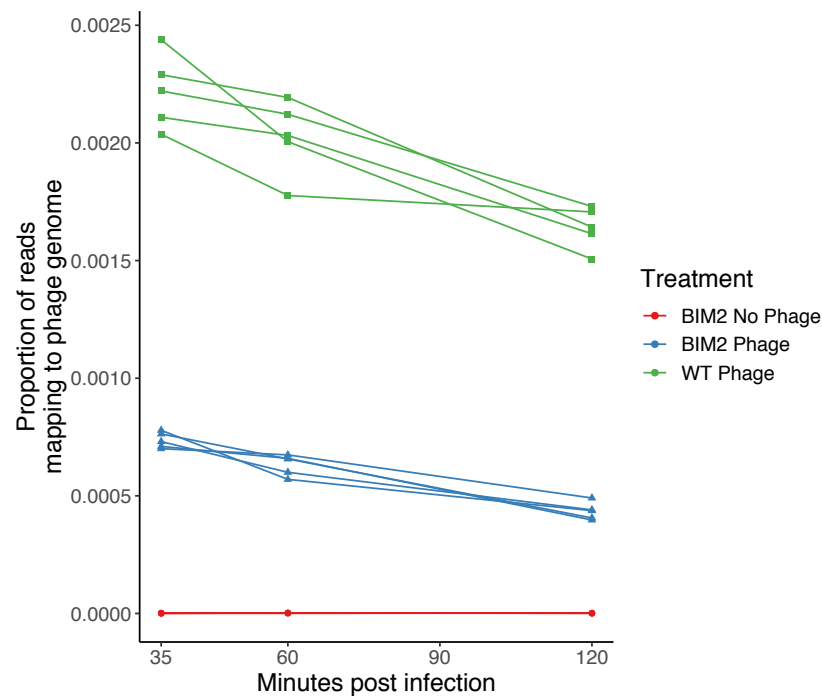757   uninfected controls (green, n = 5). Samples taken 35, 60 and 120 minutes post-infection.

758
759

760

761

762   Fig. S6.

763   Total phage gene expression following infection with 8 X 10^9 PFU DMS3vir (MOI 0.5)

764   across PA14 WT (green, n = 5), PA14 BIM2 (blue, n = 5) and PA14 BIM2 uninfected

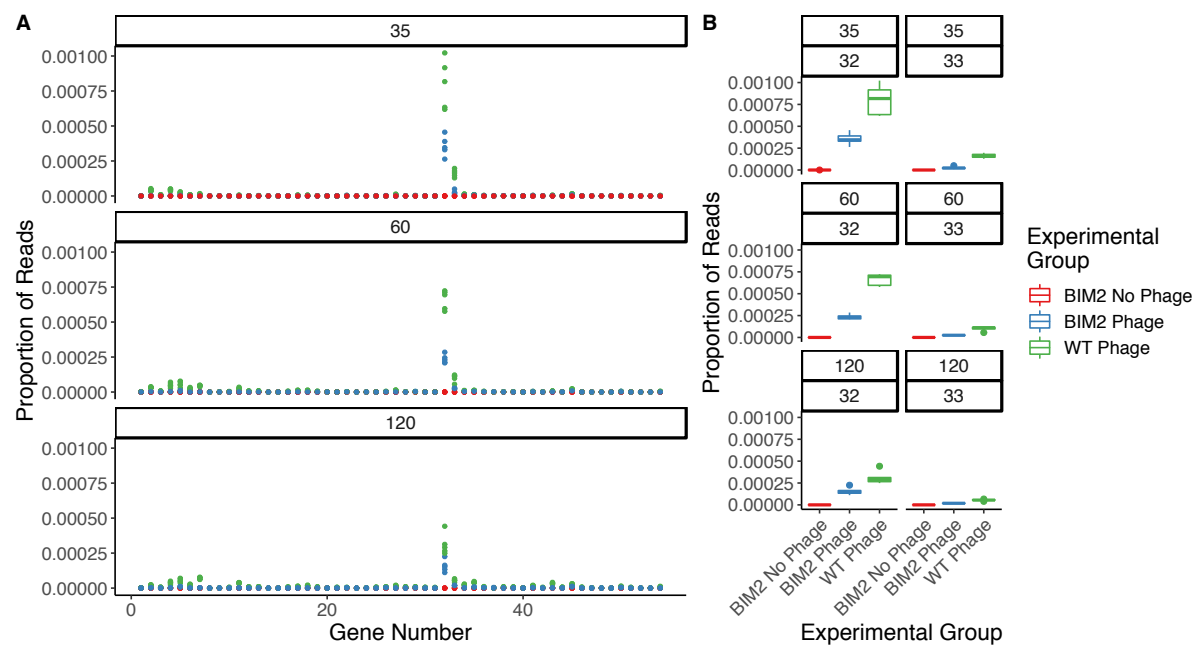765   controls (red, n = 5). Samples taken 35, 60 and 120 minutes post-infection.

766
767

768

769

770 Fig. S7

771 A) Phage gene expression of each annotated phage gene following infection with 8 X 10^9

772 PFU DMS3vir (MOI 0.5) across PA14 WT (green, n = 5), PA14 BIM2 (blue, n = 5) and

773 PA14 BIM2 uninfected controls (red, n = 5) at 35, 60 and 120 minutes post-infection. B)

774 Gene expression of the *acr* protein (32) and its *aca* repressor (33) across sampling times and

775 treatments.

776
777
778
779
780
781
782
783
784
785
786
787
788

789   Table S1

790   Post-hoc comparisons of contrasts that compare relative fitness. Numbers in the contrast

791   denote sampling time (day 4 or day 12) and the given phenotypes (CRISPR, SM or sensitive).

792

Contrast	Estimate	SE	df	t.ratio	p-value
4_CRISPR-12_CRISPR	-0.2773	0.0474	122.8124	-5.8475	**1e-04**
4_CRISPR-4_Sens	-0.1115	0.0586	109.4472	-1.9017	0.4067
4_CRISPR-12_Sens	-0.3887	0.0742	111.9035	-5.2423	**1e-04**
4_CRISPR-4_SM	-0.1243	0.0516	96.3502	-2.4093	0.1634
4_CRISPR-12_SM	-0.4015	0.0693	111.6448	-5.7951	**1e-04**
12_CRISPR-4_Sens	0.1658	0.0766	120.3732	2.1639	0.2625
12_CRISPR-12_Sens	-0.1115	0.0586	109.4472	-1.9017	0.4067
12_CRISPR-4_SM	0.153	0.0708	113.2484	2.1593	0.2652
12_CRISPR-12_SM	-0.1243	0.0516	96.3502	-2.4093	0.1634
4_Sens-12_Sens	-0.2773	0.0474	122.8124	-5.8475	**1e-04**
4_Sens-4_SM	-0.0128	0.058	108.8156	-0.2211	0.9999
4_Sens-12_SM	-0.2901	0.0754	119.9723	-3.8455	**0.0026**
12_Sens-4_SM	0.2644	0.0744	112.3086	3.5541	**0.0072**
12_Sens-12_SM	-0.0128	0.058	108.8156	-0.2211	0.9999
4_SM-12_SM	-0.2773	0.0474	122.8124	-5.8475	**1e-04**

793

794
795
796   Table S2.

797
798   Primers and PCR conditions used for amplicon sequence analysis:

CRISPR array	Primers	Sequence	PCR conditions
CRISPR 1	CR1_F CR1_R	GGCGCTGGAGCCCTTGGGGCTTGG GCGGCTGCCGGTGGTAGCGGGTG	95 C X 1 minutes 95 C X 15 seconds 69 C X 15 seconds

			72 C X 30 seconds 72 C X 7 minutes
CRISPR 2	CR2_F CR2_R	GCTCGACTACTACAACGTCCGGC GGGTTTCTGGCGGGAAAAACTCGG	95 C X 1 minutes 95 C X 15 seconds 69 C X 15 seconds 72 C X 30 seconds 72 C X 7 minutes

799

800   Table S3

801

802   Primers for cloning proteaseI gene of DMS3vir

803

Primer Name	Sequence
ProI_F	5'GCCGGAATTCGATGGAAAAGAACCGCCTACTCG
ProI_R	5'GCCGGAATTCGATGGAAAAGAACCGCCTACTCG

804

805

806

807